JBC ARTICLE

Acquisition of exogenous fatty acids renders apicoplast-based biosynthesis dispensable in tachyzoites of *Toxoplasma*

Received for publication, February 11, 2020, and in revised form, April 8, 2020 Published, Papers in Press, April 27, 2020, DOI 10.1074/jbc.RA120.013004

Xiaohan Liang[1], Jianmin Cui[1], Xuke Yang[1], Ningbo Xia[1], Yaqiong Li[1], Junlong Zhao[1,2,3], Nishith Gupta[1,4,*], and Bang Shen[1,2,*]

From the [1]State Key Laboratory of Agricultural Microbiology, College of Veterinary Medicine, Huazhong Agricultural University, Wuhan, Hubei Province, People's Republic of China, the [2]Key Laboratory of Preventive Medicine in Hubei Province, Wuhan, Hubei Province, People's Republic of China, the [3]Hubei Cooperative Innovation Center for Sustainable Pig Production, Wuhan, Hubei Province, People's Republic of China, and the [4]Department of Molecular Parasitology, Institute of Biology, Faculty of Life Sciences, Humboldt University, Berlin, Germany

Edited by Dennis R. Voelker

***Toxoplasma gondii* is a common protozoan parasite that infects a wide range of hosts, including livestock and humans. Previous studies have suggested that the type 2 fatty acid synthesis (FAS2) pathway, located in the apicoplast (a nonphotosynthetic plastid relict), is crucial for the parasite's survival. Here we examined the physiological relevance of fatty acid synthesis in *T. gondii* by focusing on the pyruvate dehydrogenase complex and malonyl-CoA-[acyl carrier protein] transacylase (FabD), which are located in the apicoplast to drive *de novo* fatty acid biosynthesis. Our results disclosed unexpected metabolic resilience of *T. gondii* tachyzoites, revealing that they can tolerate CRISPR/Cas9–assisted genetic deletions of three pyruvate dehydrogenase subunits or FabD. All mutants were fully viable in prolonged cultures, albeit with impaired growth and concurrent loss of the apicoplast. Even more surprisingly, these mutants displayed normal virulence in mice, suggesting an expendable role of the FAS2 pathway *in vivo*. Metabolic labeling of the Δ*pdh-e1α* mutant showed reduced incorporation of glucose-derived carbon into fatty acids with medium chain lengths (C14:0 and C16:0), revealing that FAS2 activity was indeed compromised. Moreover, supplementation of exogenous C14:0 or C16:0 significantly reversed the growth defect in the Δ*pdh-e1α* mutant, indicating salvage of these fatty acids. Together, these results demonstrate that the FAS2 pathway is dispensable during the lytic cycle of *Toxoplasma* because of its remarkable flexibility in acquiring fatty acids. Our findings question the long-held assumption that targeting this pathway has significant therapeutic potential for managing *Toxoplasma* infections.**

Toxoplasma gondii is an obligate intracellular protozoan infecting a variety of hosts, including 30% of the world's human population and many warm-blooded animals (1). It is an extremely successful pathogen, able to survive and propagate in virtually all nucleated cells of its host (2). One fundamental question to be addressed in the field is the metabolic strategies that allow *Toxoplasma* to survive in such diverse nutritional environments. Previous studies have demonstrated flexibility of carbon metabolism in this parasite, with it being able to use glucose, glutamine, lactate, and even amino acids as carbon sources to support its bioenergetic needs (3–5). More recently, Krishnan *et al.* (6) have constructed a curated genome-scale metabolic model, predicting additional metabolic plasticity in *T. gondii*. On the other hand, the detailed mechanisms underlying such notable metabolic flexibility are still largely unexplored.

Fatty acids (FAs) are essential to all living cells, as they have diverse biological functions ranging from energy storage to membrane biogenesis (7). All cells have evolved sophisticated approaches to satisfy their FA demands (8). Genomic analyses suggest that *Toxoplasma* has at least three potential pathways to synthesize FAs of different chain lengths (7). First, the parasite harbors a FAS1 enzyme, like its mammalian hosts, but its biochemical activity has not yet been confirmed. Second, it encodes a FAS2 pathway located in the apicoplast, which is a vestigial plastid existing in several apicomplexan parasites, including *Plasmodium* and *Eimeria* species. Third, *Toxoplasma* contains a fatty acid elongation pathway in the endoplasmic reticulum. Although the relative contribution of these pathways to net fatty acid biosynthesis has not been fully established, the current experimental data suggest that FAS2 is involved in *de novo* synthesis of medium to long acyl chains (9), whereas the fatty acid elongation pathway produces very-long-chain and unsaturated FAs (9, 10). Recent work has also shown that *Toxoplasma* can scavenge fatty acids, likely by inducing autophagy of lipid droplets in the host cell (11).

Among the aforementioned pathways of fatty acid biogenesis, FAS2 is the most extensively studied so far. It involves a series of sequential reactions catalyzed by distinct enzymes (PDH, acetyl-coenzyme A carboxylase, ACP, FabD, acyl carrier protein synthase, FabH, FabB/F, FabG, FabZ, and FabI), ultimately leading to *de novo* production of fatty acids with eight carbons or more (12, 13). FAS2 begins with production of acetyl-CoA in the apicoplast, which is believed to be catalyzed by the pyruvate dehydrogenase (PDH) complex. PDH belongs to the α-keto dehydrogenase family. It consists of four subunits, E1α, E1β, E2, and E3, which, along with respective cofactors, assemble into a complex with E1, E2, and E3 domains (14). These functional domains have pyruvate dehydrogenase, dihy-

This article contains supporting information.

* For correspondence: Bang Shen, shenbang@mail.hzau.edu.cn; Nishith Gupta, Gupta.Nishith@hu-berlin.de.

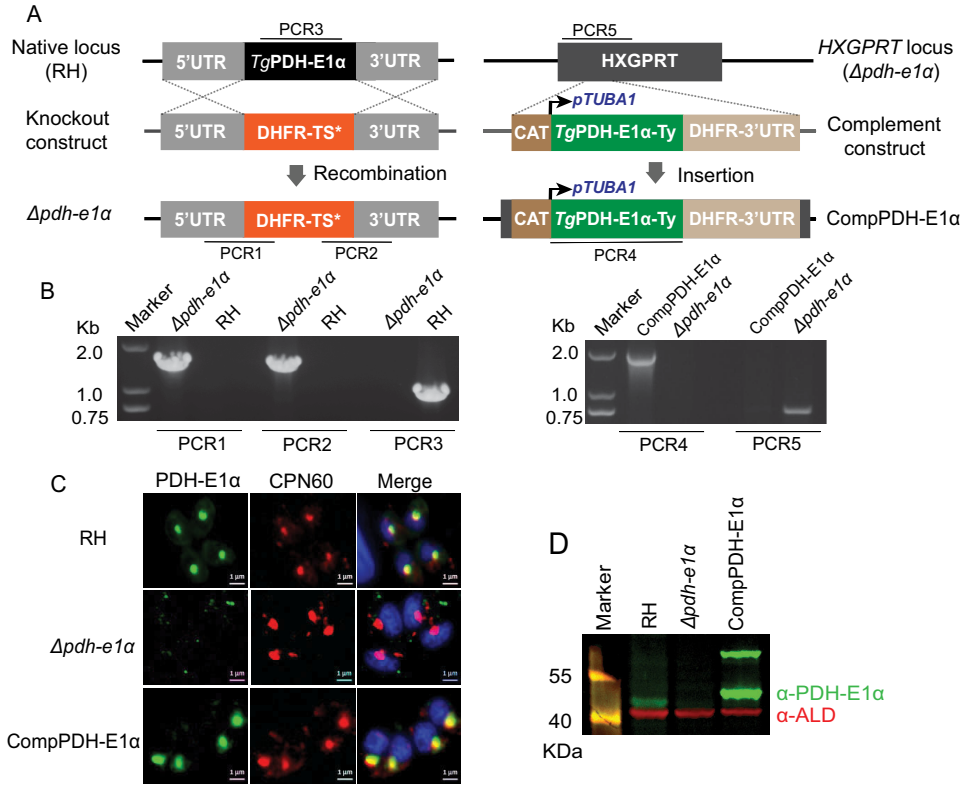

Figure 1. Construction of *Tg*PDH-E1α deletion and complementation strains. *A*, schematic showing generation of the Δ*pdh-e1α* and Δ*pdh-e1α*/PDH-E1α (CompPDH-E1α) strains via CRISPR-Cas9–assisted gene engineering. *PCR1–PCR5* indicate screening of clonal mutants. *B*, diagnostic PCRs confirming the Δ*pdh-e1α* and CompPDH-E1α strains. *C*, immunofluorescent assay showing the presence or absence of PDH-E1α. Samples were stained with anti-*Tg*PDH-E1α (which was generated from mice using a recombinant antigen corresponding to residues 158–304 of *Tg*PDH-E1α) and anti-*Tg*CPN60 antibodies. *Scale bars* = 1 μm. *D*, immunoblot checking the expression of *Tg*PDH-E1α (*green*); *Tg*ALD (*red*) was included as a loading control. The two bands for PDH-E1α in the complement strain correspond to the full-length (~70 kDa) and mature (~45 kDa, after removal of the apicoplast targeting sequence) forms of the protein.

drolipoyl transacetylase, and dihydrolipoyl dehydrogenase activity, respectively (Fig. S1*A*) (15). The entire enzyme complex catalyzes net conversion of pyruvate into acetyl-CoA, CO_2, and NADH.

PDH is critical for carbon homeostasis and energy production in most eukaryotic cells (16), which have mitochondrion-dwelling PDH to link cytoplasmic glycolysis and the mitochondrial TCA cycle (17). Plant cells have a second PDH complex, located in the plastid, where it catalyzes production of acetyl-CoA from pyruvate to initiate *de novo* synthesis of fatty acids (18). Notably, Apicomplexa parasites like *Toxoplasma* express only one PDH complex in the apicoplast (14, 19), where it is thought to convert pyruvate to acetyl-CoA to fuel FAS2. On the other hand, these parasites have repurposed a branched-chain keto-acid dehydrogenase complex to perform the catalytic function of PDH in the mitochondrion (20). Genetic ablation of branched-chain keto-acid dehydrogenase–E1α is detrimental to the virulence of *Toxoplasma* and *Plasmodium* parasites due to impaired flux of glucose-derived carbon into the TCA cycle.

Because host cells do not have an apicoplast or the FAS2 pathway, the latter is considered an excellent drug target against apicomplexan parasites (21). Several chemicals inhibiting FAS2 enzymes have been shown to have anti-malarial, anti-toxoplasmosis, and/or anti-neosporosis activities (22). Genetic studies of *Plasmodium* species suggest that the importance of FAS2 differs at different stages of the life cycle (12, 23, 24). In contrast, conditional depletion of the ACP remains the only genetic evidence to infer the importance of FAS2 in *Toxoplasma*. Knockdown of ACP results in reduced lipoylation of PDH, loss of the apicoplast, growth arrest in culture, and strong attenuation of virulence, suggesting a critical role of FAS2 in *Toxoplasma* (21). This study examined the physiological importance of PDH and FabD, revealing unprecedented plasticity in fatty acid biogenesis of *T. gondii*.

Results

The TgPDH complex in the apicoplast originated from cyanobacteria

The parasite genome encodes five genes annotated as PDH subunits: E1α, E1β, E2, E3-I, and E3-II. Previous work using ectopic expression of epitope-tagged PDH subunits as well as sera against native proteins showed apicoplast localization of the E1β and E2 subunits (19). We started our work by confirming the subcellular location of PDH through C-terminal tagging of each endogenous protein (Fig. S1*B*). A spaghetti monster HA (smHA) epitope (25) was fused to the C terminus of each subunit at the endogenous locus using CRISPR-Cas9–mediated site-specific integration in the RH Δ*ku80* strain (26). PCR confirmed the desired integration of the smHA tag in each transgenic strain. Immunofluorescent staining showed that *Tg*PDH-E1α, *Tg*PDH-E1β, *Tg*PDH-E2, and *Tg*PDH-E3-I were

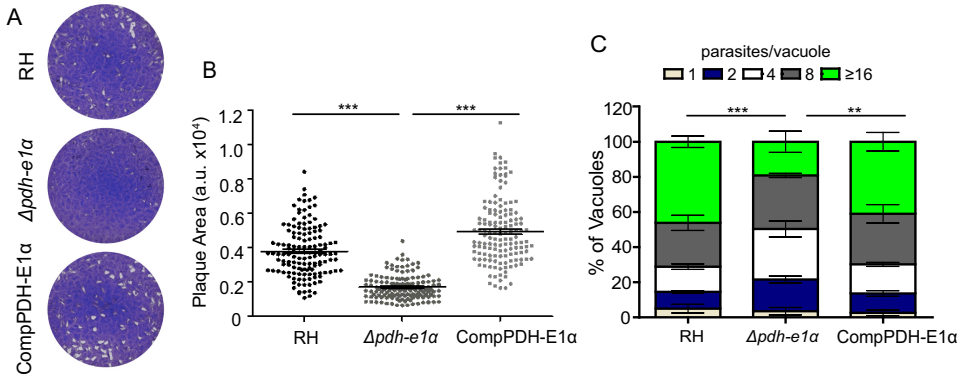

Figure 2. Loss of *Tg*PDH-E1α impairs the parasite growth. *A*, plaques showing comparative growth of the indicated strains. *B*, plaque size presented as arbitrary units (*a.u.*). Means ± S.E. of >120 plaques from three independent assays (***, $p < 0.001$; one-way ANOVA with Bonferroni's post-test). *C*, Replication rates of depicted strains (24 h post-infection). Means ± S.E. from three independent experiments (**$p < 0.01$, ***$p < 0.001$, two-way ANOVA with Bonferroni's post-test).

expressed in the apicoplast, as indicated by colocalization with the organelle marker *Tg*CPN60. On the other hand, *Tg*PDH-E3-II colocalized with the mitochondrial marker *Tg*HSP60 (Fig. S1*C*).

We next examined the evolutionary origin of all PDH subunits by phylogenetic analyses of their peptide sequences (Fig. S2). Phylograms constructed for individual *Tg*PDH subunit revealed that E1α, E1β, E2, and E3-I segregated with corresponding plastid and cyanobacterial PDH counterparts, whereas E3-II showed a distinct cladding pattern with mitochondrial and bacterial PDH-E3 (Fig. S2). These results suggest that the former four subunits are derived from cyanobacteria via secondary symbiosis, similar to *Plasmodium* PDH subunits (14), and the hosting organelle apicoplast itself (27). Our phylogenetic analyses in conjunction with the aforementioned localization studies also suggest that the E1α, E1β, E2, and E3-I subunits form a functional PDH complex located in the apicoplast, whereas E3-II is likely a component of the mitochondrial dehydrogenase complex.

TgPDH-E1α supports parasite growth but is not needed for survival

To evaluate the physiological importance of *Tg*PDH, we first knocked out the E1α subunit in the RH strain. The entire coding region of the *Tg*PDH-E1α gene was replaced by the *DHFR-TS** selection marker, which confers pyrimethamine resistance (Fig. 1*A*). Diagnostic PCRs were used to screen single clones lacking *TgPDH-E1α* (Fig. 1*B*). Immunostaining confirmed disruption of *Tg*PDH-E1α in the deletion mutants (Fig. 1, *C* and *D*). Unlike the parental strain, *Tg*PDH-E1α was not detectable in the Δ*pdh-e1α* strain. The Δ*pdh-e1α* mutant grew slower in routine culture. Indeed, in plaque assays, which indicate the overall fitness of the parasites, the Δ*pdh-e1α* mutant produced significantly smaller plaques than the parental strain, although the number of plaques seemed to be similar (Fig. 2, *A* and *B*). The replication assay also demonstrated a slower proliferation rate of the Δ*pdh-e1α* strain. The fraction of parasitophorous vacuoles with 16 or more parasites was considerably lower in the mutant than in the parental strain (Fig. 2*C*). On the other hand, host cell invasion and ionophore (A23187)–induced egress were not affected by inactivation of *PDH-E1α* (Fig. S3). Taken together, these results reveal that the E1α subunit of *Tg*PDH is required for optimal growth of *T. gondii* tachyzoites *in vitro*, but it is not essential for parasite survival.

To confirm whether the growth defect observed in the Δ*pdh-e1α* mutant was a direct consequence of PDH-E1α inactivation, we complemented the Δ*pdh-e1α* strain with C-terminally Ty-tagged *Tg*PDH-E1α expressed from the *HXGPRT* locus (Fig. 1*A*). Screening PCRs confirmed the desired integration of the complementing construct (Fig. 1*B*). Immunostaining demonstrated that the ectopic PDH-E1α was successfully expressed and localized to the apicoplast, just like the endogenous protein (Fig. 1, *C* and *D*). Phenotypic analysis of the PDH-E1α–complemented strain showed restoration of the observed defects in the Δ*pdh-e1α* mutant (Fig. 2), confirming that PDH-E1α is indeed required for robust growth of the parasites.

Fatty acid synthesis is impaired in the Δpdh-e1α mutant

To determine the underlying basis of compromised growth in the Δ*pdh-e1α* strain, we estimated *de novo* fatty acid synthesis by testing the flux of [$^{13}C_6$]glucose-derived carbon (Fig. 3*A*). Intracellular parasites of the parental and mutant strains were labeled with [$^{13}C_6$]glucose for 48 h, and subsequent incorporation of sugar-derived carbon (^{13}C) into fatty acids was assessed by GC-MS. Our choice of labeling intracellular parasites was based on earlier work, which demonstrated that fatty acid synthesis is negligible in the extracellular stage (4). We found that the Δ*pdh-e1α* mutant showed reduced ^{13}C-labeling of fatty acids compared with the parental strain. The extent of tracer incorporation differed the most for myristic (C14:0) and palmitic (C16:0) acids. *PDH-E1α* deletion led to decreased incorporation of ^{13}C into C14:0 and C16:0 (Fig. 3, *A–C*). Isotopologue profiling of myristic acid showed a significant amount of m12, m13, and m14 isotopomers (corresponding to 12, 13, and 14 carbons labeled with ^{13}C) in the parental strain, whereas the majority of them were in the m0 fraction (*i.e.* no ^{13}C labeling) in the Δ*pdh-e1α* mutant (Fig. 3*B*). A similar pattern of isotopologue abundance was also found in palmitic acid (Fig. 3*C*), suggesting a contribution of PDH to flux of glucose-derived carbon into medium-chain fatty acids. Because these two fatty acids are believed to be produced mainly in the apicoplast by FAS2 (9), our data indicate a critical role of PDH in *de novo* fatty acid

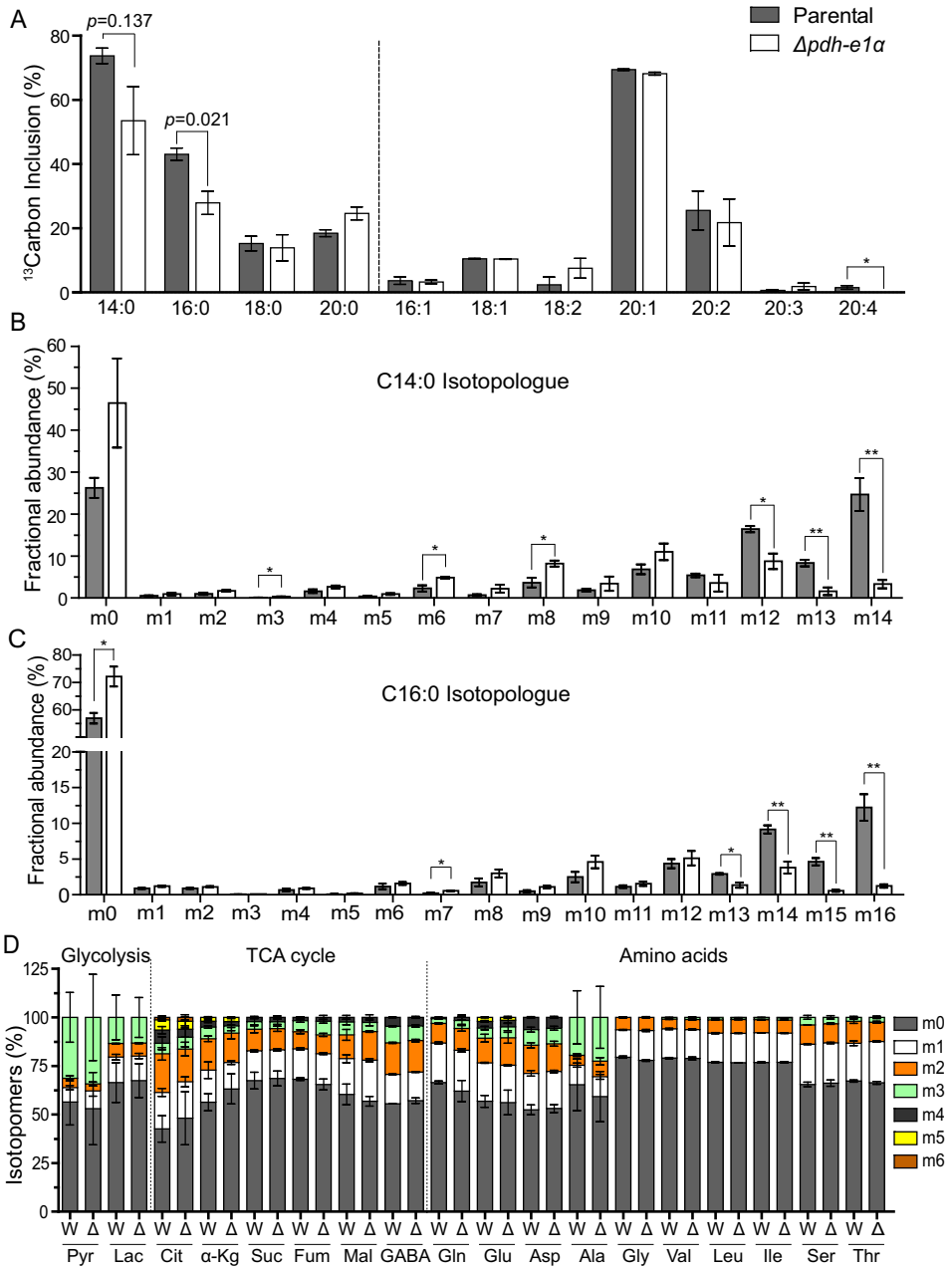

Figure 3. The Δ*pdh-e1α* strain exhibits reduced fatty acid synthesis. *A–C*, intracellular tachyzoites of the parental and Δ*pdh-e1α* strains were labeled with [$^{13}C_6$]glucose for 48 h. Subsequently, fatty acids were extracted from host-free parasites, and the relative abundance of isotopologues was assessed by GC-MS. Means ± S.E. from three experiments (*, $p < 0.05$; **, $p < 0.01$; Student's *t* test). *A*, overall fraction of ^{13}C-labeled fatty acids regardless of the number of carbons that were labeled. *B* and *C*, ^{13}C inclusion in isotopologues of myristic acid (C14:0) and palmitic acid (C16:0). *D*, flux of [$^{13}C_6$]glucose-derived tracer carbon into glycolysis and TCA cycle metabolites and amino acids. Extracellular parasites were labeled with [$^{13}C_6$]glucose for 4 h, followed by metabolite extraction and GC-MS analysis. *W*, RH; Δ, Δ*pdh-e1α*; *Pyr*, pyruvate; *Lac*, lactate; *Cit*, citrate; *α-Kg*, α-ketoglutarate; *Suc*, succinate; *Fum*, fumarate; *Mal*, malate.

synthesis. We also performed [$^{13}C_6$]glucose labeling in extracellular parasites (4 h) to examine carbon flux into glycolysis, the TCA cycle, and amino acids. None of these pathways were affected by *PDH-E1α* disruption (Fig. 3*D*), as expected.

A somewhat selective reduction in synthesis of C14:0 and C16:0 in the Δ*pdh-e1α* strain prompted us to restore the mutant's growth by addition of exogenous C14:0 and C16:0. Plaque and replication assays were performed in the absence or presence of 100 μM myristic acid, palmitic acid, or a mixture of both (50 μM each). Supplementation indeed improved growth of the Δ*pdh-e1α* mutant, as shown by an almost 50% increase in plaque size with either fatty acid (Fig. 4, *A* and *B*). This finding was further supported by replication rates that were significantly increased in the mutant upon addition of fatty acids (Fig. 4*C*). An additive effect on the mutant's growth was also apparent when both acyl chains were provided simultaneously. Collectively, these experiments demonstrate the functional importance of PDH-E1α for fatty acid biogenesis, likely in the apicoplast.

The E2 and E3-I subunits of the PDH complex are dispensable

To consolidate the above results, we constructed two additional mutants lacking the E2 or E3-I subunits of the PDH complex, utilizing a similar homologous gene replacement strategy as shown in Fig. 1*A*. Genes encoding the E2 or E3-I subunits

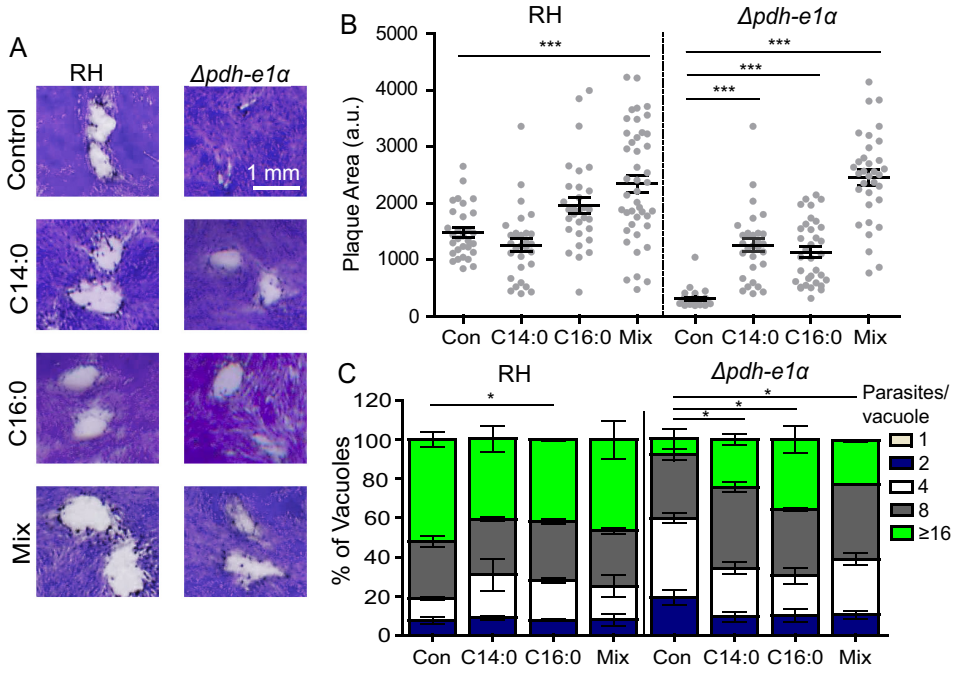

Figure 4. Exogeneous fatty acid supplementation partially restores the growth defect in the Δ*pdh-e1α* mutant. *A*, plaque assays in the absence (*Control*) or presence of 100 μM myristic (C14:0) or palmitic acid (C16:0) or their mixture (*Mix*, 50 μM myristic acid + 50 μM palmitic acid). *B*, plaque sizes obtained from *A* (arbitrary units (*a.u.*)). Data represent means ± S.E. of more than 120 plaques from three experiments (***, $p < 0.001$; one-way ANOVA with Bonferroni's post-test). *Con*, control. *C*, replication assays upon addition of the indicated fatty acids. Means ± S.E. of 150 vacuoles from three assays (*, $p < 0.05$; two-way ANOVA with Bonferroni's post-test).

were completely replaced by the *DHFR-TS** selection marker. Screening PCRs confirmed successful deletion of individual genes in corresponding mutants (Fig. 5, *A* and *B*). The Δ*pdh-e2* mutant was further ascertained by immunostaining and immunoblot analyses (Fig. 5, *C* and *D*). The Δ*pdh-e2* and Δ*pdh-e3-I* strains displayed reduced growth in plaque and proliferation assays (Fig. 6, *A* and *B*), phenocopying the Δ*pdh-e1α* mutant (Fig. 2). Nonetheless, the Δ*pdh-e2* and Δ*pdh-e3-I* mutants were viable in prolonged cultures, suggesting that neither subunit is essential for tachyzoites.

PDH is dispensable for the parasite virulence

Our results strongly assert that the parasite can tolerate the absence of the PDH complex, albeit with impaired reproduction *in vitro*. To examine the *in vivo* relevance, we infected ICR mice with the abovementioned mutants lacking individual PDH subunits and subsequently scored the survival of infected animals. Surprisingly, although all three PDH-deficient mutants had a variable degree of growth defects in culture, none of them showed evidence of attenuated virulence in mice (Fig. 6*C*). In all cases, parasitized animals succumbed to death within 10–12 days of infection, suggesting complete dispensability of the PDH complex for parasite virulence while questioning the significance of the FAS2 pathway during acute infection with *T. gondii*.

PDH mutants show loss of the apicoplast correlated with their growth phenotypes

Interruption of metabolic processes in the apicoplast is typically associated with its loss over time, as reported for the ACP depletion mutant (21). We therefore examined the integrity of the apicoplast in the above PDH mutants. The Δ*pdh-e1α*, Δ*pdh-e2*, and Δ*pdh-e3-I* strains were subjected to immunostaining of the organelle marker *Tg*CPN60. In the parental strain, nearly all parasites harbored an apicoplast, as indicated by the bright *Tg*CPN60 signal (Fig. 7*A*). In the PDH deletion mutants, however, the integrity of the apicoplast varied. The Δ*pdh-e2* mutant did not seem to show significant defects in apicoplast maintenance, as judged by strong *Tg*CPN60 staining in most tachyzoites (Fig. 7, *A* and *B*). The Δ*pdh-e1α* mutant experienced modest apicoplast loss, in which about 15% parasites did not have detectable *Tg*CPN60. The Δ*pdh-e3-I* mutant displayed the most dramatic phenotype, with almost 50% of parasites devoid of *Tg*CPN60 signal. The degree of apicoplast loss in individual mutants correlated well with the growth defects in plaque assays.

The apicoplast integrity in the PDH mutants was also assessed using an anti-*Tg*PYK2 antibody. In the parental (RH) strain, *Tg*PYK2 was mainly localized in the apicoplast, although it also displayed weak staining in vesicle-like structures. In contrast, in the *PDH-E1α* and *PDH-E2* knockout mutants, *Tg*PYK2 signal in the apicoplast was reduced, and increased staining of vesicle-like structures was observed (Fig. S4). Such a shift of the PYK2 staining signal was even more evident in the Δ*pdh-e3-I* mutant, half of which had *Tg*PYK2 detectable only in vesicle-like structures but not in the apicoplast (Fig. S4). These results confirmed our aforementioned observations with *Tg*CPN60 staining. Although the basis of such differential apicoplast loss in different PDH mutants is inexplicable, our results suggest a role of PDH in maintenance of this organelle.

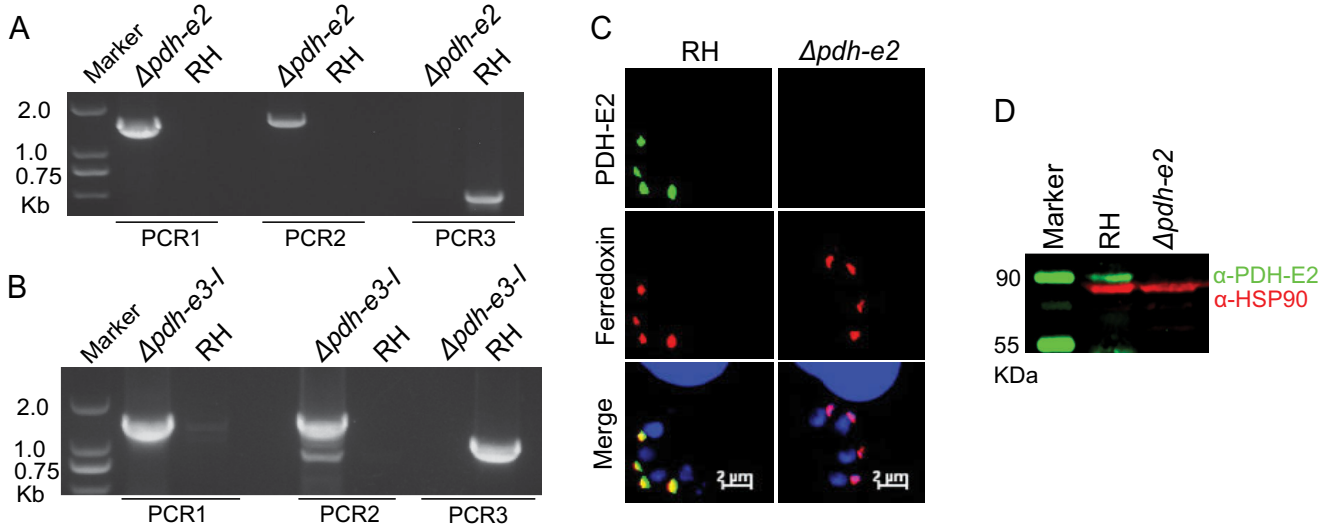

Figure 5. Tachyzoites can tolerate ablation of the *Tg*PDH-E2 and E3-I subunits. *A* and *B*, PCR screening of selected clones of the Δ*pdh-e2* or Δ*pdh-e3-I* strains. *C* and *D*, loss of PDH-E2 expression in the Δ*pdh-e2* mutant, as deduced by immunofluorescent staining (*C*) and Western blotting (*D*).

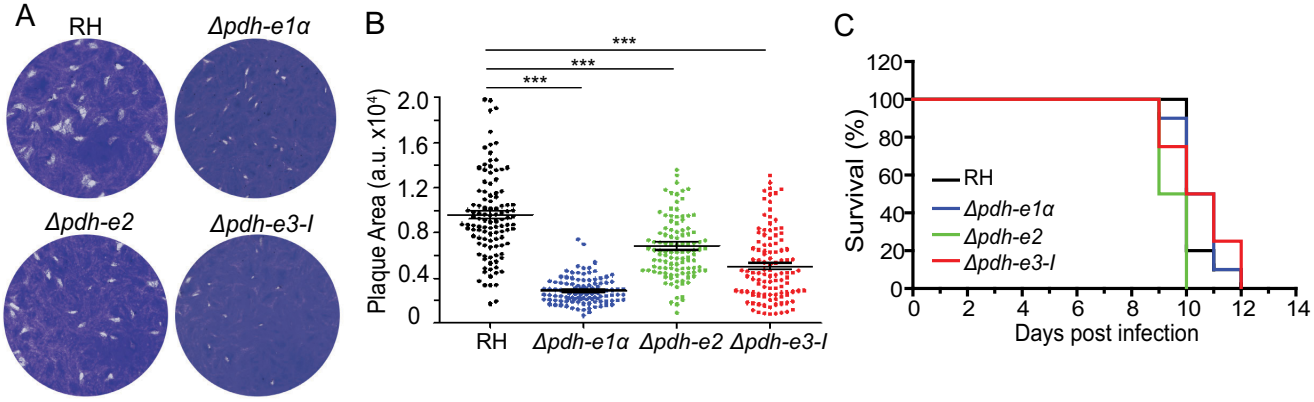

Figure 6. PDH-deficient mutants are viable *in vitro* and fully virulent in mice. *A*, plaque assays comparing overall growth of the indicated strains. *B*, relative size of plaques in *A* (means ± S.E. of more than 120 plaques from three assays; ***, $p < 0.001$; one-way ANOVA with Bonferroni's post-test). *a.u.*, arbitrary units. *C*, survival rates of mice infected with the parental and mutant strains.

Deletion of FabD confirms nonessentiality of the FAS2 pathway

The genetic disruption of three PDH subunits indicated that FAS2 is dispensable, which is in contrast to a previous report of conditional depletion of ACP (21). We therefore revisited the physiological significance of FAS2 by targeting the *FabD* enzyme, which catalyzes transfer of the malonyl group from malonyl-CoA to ACP to produce malonyl-ACP. The latter serves as the carbon donor for the elongation cycles of FAS2. Interestingly, *FabD* was readily knocked out in the type 1 RH strain (Fig. 8*A*). Plaque and replication assays demonstrated that Δ*fabD* mutants also exhibited noticeable growth defects (Fig. 8, *B* and *D*), which could be restored by complementation. Moreover, although some Δ*fabD*-infected animals survived slightly longer than the control group, the virulence of the Δ*fabD* mutant was not significantly different from that of the parental strain (Fig. 8*E*). These phenotypes resonate well with that of the PDH-deficient mutants. Hence, these results together show that the FAS2 pathway is indeed not essential in tachyzoites.

Discussion

PDH is a central enzyme complex in carbon metabolism that converts glycolysis-derived pyruvate into acetyl-CoA (16). In apicomplexan parasites, there is only one PDH complex, which is localized in the apicoplast instead of the mitochondrion (12). The apicoplast is a unique organelle in most apicomplexan parasites that houses many important metabolic pathways, including fatty acid synthesis (27). The PDH complex is believed to produce acetyl-CoA, which is required by the FAS2 pathway in the apicoplast of *T. gondii* (14). According to a previous report (21), depletion of ACP (a core component of FAS2) severely reduced parasite growth in plaque assays and attenuated virulence in mice, implying an essential nature of FAS2 in the apicoplast. Accordingly, the PDH complex was also expected to be vital for the lytic cycle. Unexpectedly, however, we discovered that, despite a slower growth phenotype *in vitro*, mutants lacking the E1α, E2, and E3-I subunits of *Tg*PDH are viable in prolonged cultures and fully virulent in mice, demonstrating dispensability of PDH for parasite survival and virulence. The viability of PDH-deficient mutants also suggests nonessential-

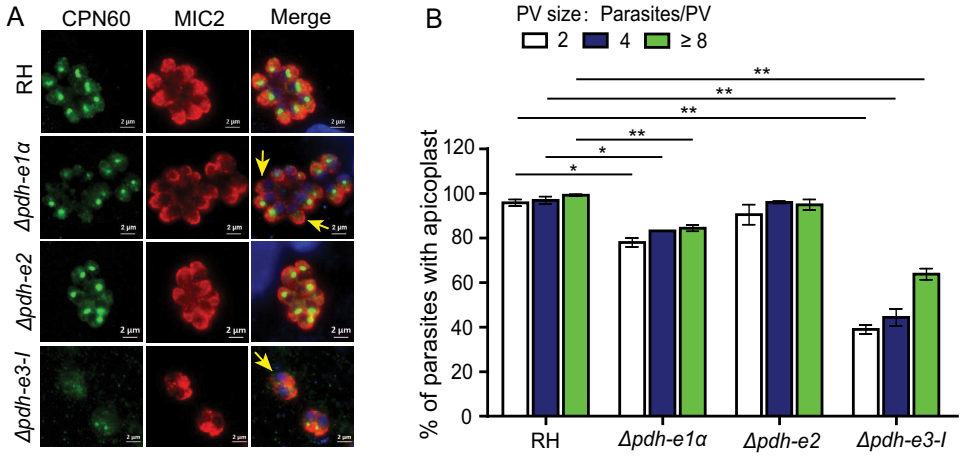

Figure 7. Assessment of apicoplast integrity in PDH mutants. *A*, immunofluorescent staining of the apicoplast-specific marker *Tg*CPN60. *Yellow arrows* indicate parasites with no evident apicoplast staining. *Scale bars* = 2 μm. *B*, quantification of apicoplast from *A*. The percentage of parasites with apicoplasts in parasitophorous vacuoles (*PVs*) of different sizes was determined by *Tg*CPN60 and *Tg*MIC2 staining (means ± S.E. of 150 vacuoles, $n = 3$ assays; *, $p < 0.05$; **, $p < 0.01$; Student's *t* test).

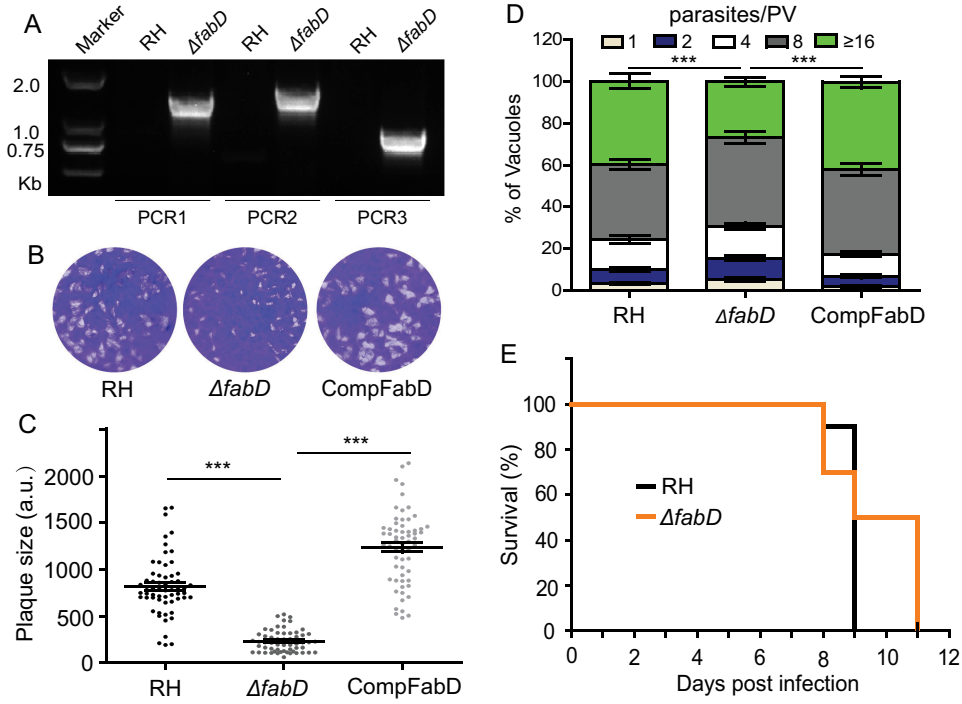

Figure 8. FabD deletion mutants are viable in culture and virulent in mice. *A*, screening PCR confirmed successful replacement of *FabD* by the selection marker in Δ*fabD*. *B*, plaque assay of the indicated strains. *C*, relative size of plaques in *B* (means ± S.E.; $n = 2$ assays, each with 3 replicates; ***, $p < 0.001$; one-way ANOVA with Bonferroni's post-test). *D*, intracellular replication (24 h) assay (***, $p < 0.001$, two-way ANOVA with Bonferroni's post-test). *E*, survival of mice infected with the indicated strains.

ity of FAS2. These results were confirmed by the Δ*fabD* mutant, which was also viable in sustained culture and fully virulent in mice.

In further work, we demonstrated a role of the PDH complex in *de novo* fatty acid synthesis. Among different subunits of the PDH complex, E1α and E1β form a heterotetrameric E1 domain that catalyzes decarboxylation of pyruvate to initiate the whole reaction catalyzed by PDH (15). We characterized the Δ*pdh-e1α* mutant to decipher the function of PDH in *T. gondii*. When labeled with [$^{13}C_6$]glucose, the flux of sugar-derived carbon into myristic acid (C14:0) and palmitic acid (C16:0) declined significantly in the Δ*pdh-e1α* strain. C14:0 and C16:0 are primarily produced by FAS2 (7). Therefore it can be argued that *Tg*PDH activity supports acyl chain synthesis in the apicoplast and that reduced FAS2 activity upon deletion of PDH-E1α underlies the growth defect. Conversely, growth of the Δ*pdh-e1α* mutant was improved by supply of exogenous fatty acids, suggesting that *T. gondii* can salvage fatty acids from the environment, although the detailed mechanisms warrant further investigation. The salvage and *de novo* synthesis pathways may cooperate to ensure fatty acid biogenesis under diverse conditions.

Notably, deletion of *PDH-E1α* did not completely abolish the flux of [$^{13}C_6$]glucose-derived carbon into C14:0 and C16:0 acyl

chains (Fig. 3, *A–C*), which can be explained as follows. Because metabolic labeling was performed with parasites replicating in host cells, there may have been a contribution of host components in our parasite samples. Moreover, salvage of host-derived fatty acids may be induced upon deletion of *PDH-E1α*. Likewise, we cannot rule out a contribution of the FAS1 pathway in the parasite, although its activity has not yet been reported. Last but not least, PDH may not be the only source of acetyl-CoA in the apicoplast. There are acetyl-CoA pools in the parasite cytosol and mitochondrion that may fuel the apicoplast with acetyl-CoA, although there is no reported apicoplast-localized acetyl-CoA transporter. Nonetheless, considering such additional sources of acetyl-CoA, we deleted *FabD* to examine the actual significance of FAS2. Because the *PDH* and *FabD* deletion mutants phenocopied each other, we believe that even if there is yet another source of acetyl-CoA for the apicoplast, its contribution to the FAS2 pathway is probably rather minor.

The phenotypes of the *PDH/FabD* deletion mutants are not fully consistent with that of the mutant depleted with ACP (21). Although these strains showed impaired growth *in vitro*, the most obvious difference is their virulence. The ACP knockdown strain is highly attenuated in mice whereas PDH/FabD-null mutants are not. Such discrepancies may be explained by the following. *Tg*ACP may have other crucial roles beyond its core function as an acyl carrier protein. In this regard, *Pf*ACP has already been shown to have acylation and malonyl-transferase activities, which may contribute to the apicoplast metabolism beyond FAS2 (29, 30). Given the conservation, *Tg*ACP could exhibit similar activities. The ACP depletion mutant was engineered in the TATi strain, which itself is highly attenuated in mice for unknown reasons. Therefore, it is difficult to draw solid conclusions regarding the effect of ACP knockdown on parasite virulence using this strain. On the other hand, using clean genetic knockouts, our results have clearly shown that PDH and FabD are important but dispensable for parasite virulence. The recent work of Krishnan *et al.*(6) regarding FabZ is consistent with the data reported here.

Since its identification, FAS2 has been studied extensively in malaria parasites as a potential drug target. However, more recent work using gene deletion mutants (FabI, FabB/F, and FabZ, etc.) demonstrated that FAS2 is dispensable for blood-stage parasites but critical for mosquito or liver-stage developments (12, 23, 24). The dispensability of FAS2 for blood-stage *Plasmodium* is explained by their ability to scavenge fatty acids from red blood cells (24). Consistently, *Plasmodium* species lacking PDH subunits show normal erythrocytic development but growth defects during the hepatic or mosquito stages (23, 31, 32). Similarly, FAS2 in *Toxoplasma* may have more important roles in other stages, such as during sporulation, when the parasite undergoes extensive membrane synthesis but does not have access to host-derived resources. At least the tachyzoite stage has multiple routes to acquire fatty acids, which render *de novo* synthesis dispensable, questioning the long-believed potential of FAS2 as an antiparasitic drug target.

Experimental procedures

Biological resources and reagents

Type I RH and its derivative strains as well as the PDH and FabD deletion mutants generated here were propagated in human foreskin fibroblast cells (ATCC), as described elsewhere (33). Anti-Ty (mouse), anti-*Tg*SAG1 (mouse), anti-*Tg*MIC2 (mouse), and anti-*Tg*ALD (rabbit) antibodies were provided by David Sibley (Washington University, St. Louis, MO). Anti-*Tg*CPN60 (rabbit) was provided by Honglin Jia (Harbin Veterinary Research Institute). Anti-*Tg*PDH-E2 (mouse) was donated by Wolfgang Bohne (University of Göttingen, Göttingen, Germany). Anti-HA (rabbit) was purchased from Medical & Biological Laboratories Co.

Plasmid construction

All primers used in this study are listed in Table S1. Locus-specific CRISPR constructs were generated by replacing the *UPRT*-targeting guide RNA in pSAG1-Cas9-U6-sgUPRT with gene-specific guide RNAs, following a protocol described elsewhere (33, 34). Homology templates used for gene replacements (pPDH-E1α::DHFR-TS*, pPDH-E2::DHFR-TS*, pPDH-E3-I::DHFR-TS*, and pFabD::DHFR-TS*) were constructed by multifragment cloning using the ClonExpress MultiS Cloning Kit (Vazyme Biotech, Nanjing, China). Briefly, the 5′ and 3′ homology arms of each gene (~1 kb) were amplified from the genomic DNA of the RH strain and cloned into the pUC19 vector along with the pyrimethamine selection cassette *DHFR-TS**. The latter was amplified from pUPRT-DHFR-D (34). To make the complementation constructs pComp-PDH-E1α and pComp-FabD, *Tg*LDH1 was replaced in pCom-LDH1 (35) with the epitope-tagged coding sequence of *Tg*PDH-E1α or *FabD*, respectively.

Generation of transgenic parasites

Endogenous tagging was performed as described previously (36). The 3′ genomic tagging cassette (smHA epitope and *DHFR-TS** selection marker) flanked by gene-specific homology arms (50 bp) was amplified from the *pSL24m-Linker-smFP-DHFR-LoxP-T7* plasmid (25) using the indicated primers (Table S1). Amplicons were then cotransfected into RH Δ*ku80* along with a CRISPR plasmid targeting the 3′ UTR of the gene of interest (26). Transfected cells were selected with 1 μM pyrimethamine (Sigma-Aldrich), followed by PCR screening and immunostaining.

The Δ*pdh-e1α*, Δ*pdh-e2*, Δ*pdh-e3-I*, and Δ*fabD* mutants were constructed by CRISPR-Cas9–assisted homologous recombination as described earlier (33, 34). Briefly, the gene-specific CRISPR plasmid was cotransfected with homologous donor amplicons into freshly purified tachyzoites and then selected with pyrimethamine as mentioned above. Subsequently, clonal mutants were isolated and identified by PCR screening and immunostaining. The PDH-E1α and FabD complement strain was generated by cotransfecting the *HXGPRT*-specific (for PDH-E1α complementation) or *UPRT*-specific (for FabD complementation) CRISPR plasmids along with the PDH-E1α- or FabD-expressing cassettes into the correspond-

ing mutants and selected with 30 μM chloramphenicol (Sigma-Aldrich).

Phenotypic analysis of parasites

Plaque assays were performed as described previously (34). Similarly, invasion, replication, and egress assays were executed according to established protocols (35, 37). To test virulence, 7-week-old female ICR mice (Hubei Provincial Center of Disease Control and Prevention) were infected by intraperitoneal injection of the indicated strains (100 tachyzoites/mouse). Infected animals were monitored daily for symptoms and survival over time. All animal experiments were approved by the Ethics Committee of Huazhong Agricultural University (Permit HZAUMO-2017-029).

Metabolite measurements by GC-MS

To analyze fatty acids, intracellularly proliferating parasites were cultured in medium containing 8 mM [$^{13}C_6$]glucose (Sigma Aldrich) for 48 h. Tachyzoites were purified from host cells by 3.0-μm filtration, and samples (2.5×10^7 cells) were lysed in 1 ml of ice-cold methyl alcohol (50%) and then ultrasonicated (5 pulses of 1 min, each with a 1-min interval), followed by centrifugation ($1.6 \times 10^4 \times g$, 4 °C, 15 min). Subsequently, 800 μl of supernatant and 10 μl of internal standard (250 μg/ml nonadecanoic acid) were mixed and methylated overnight in Polytetrafluoroethylene screw-cap glass vials with 1 ml of 10% methanolic acetyl-chloride and 250 μl of *n*-hexane at room temperature. Then 5 ml of 6% potassium carbonate solution was added, and 150 μl of the *n*-hexane layer was transferred to a glass vial. Soon thereafter, 20 mg of anhydrous sodium sulfate was added to eliminate any trace of water, followed by transfer of a 60-μl sample for GC-MS (38).

To examine other metabolites, fresh extracellular tachyzoites (2.5×10^7) were labeled with 8 mM [$^{13}C_6$]glucose in glucose-free DMEM for 4 h. Parasites were pelleted and lysed in 1 ml of ice-cold methyl alcohol (50%), as mentioned above. Chloroform (0.8 ml) was added, and samples were vortexed for 30 s. The mixture was subjected to ultrasonication (5 cycles of 1 min, each with a 1-min interval), and samples were centrifuged ($1.6 \times 10^4 \times g$, 4 °C, 15 min). 700 μl of supernatant and 10 μl of internal standard (50 μg/ml L-norleucine) were mixed, followed by evaporation to dryness under a nitrogen stream. The dry residue was reconstituted in 30 μl of 20 mg/ml methoxyamine hydrochloride in pyridine, and the resulting mixture was incubated at 37 °C for 90 min. Finally, 30 μl of N-tert-Butyldimethylsilyl-N-methyltrifluoroacetamide (containing 1% Tert-butyldimethylsilyl) was added into the mixture and derivatized at 55 °C for 60 min before GC-MS. Instrument analysis was performed as described previously (35).

Data analysis and statistics

All experiments were performed at least three independent times unless specified otherwise. Data plotting and statistical analysis, as indicated in the figure legends, were done using GraphPad Prism (GraphPad Software Inc.).

Data availability

All data used in this work are contained within the manuscript.

Acknowledgments—We thank the *Toxoplasma* community for sharing resources and Shanghai Profleader Biotech Co. for GC-MS measurements.

Author contributions—X. L. and J. C. data curation; X. L., J. C., and N. G. formal analysis; X. L., J. C., X. Y., and Y. L. investigation; X. L., J. C., X. Y., and N. X. methodology; X. L. writing-original draft; N. X. and B. S. conceptualization; J. Z. and B. S. resources; J. Z. and N. G. supervision; J. Z., N. G., and B. S. funding acquisition; J. Z., N. G., and B. S. project administration; N. G. and B. S. writing-review and editing.

Funding and additional information—This work was supported by National Key Research and Development Program of China Grant 2017YFD0501304, National Natural Science Foundation of China Grant 31872463, and Fundamental Research Funds for the Central Universities in China Grant 2662019PY079. The work performed by X. L. and B. S. during their visits to the Gupta laboratory was sponsored by German Research Foundation (DFG) Grants GU1100/15 and GU1100/16.

Conflict of interest—The authors declare that they have no conflicts of interest with the contents of this article.

Abbreviations—The abbreviations used are: FA, fatty acid; PDH, pyruvate dehydrogenase; ACP, acyl carrier protein; FabD, malonyl-CoA-[acyl carrier protein] transacylase; smHA, spaghetti monster HA; TCA, tricarboxylic acid; ANOVA, analysis of variance.

References

1. Jones, J. L., and Dubey, J. P. (2012) Foodborne toxoplasmosis. *Clin. Infect. Dis.* **55,** 845–851 CrossRef Medline
2. Elmore, S. A., Jones, J. L., Conrad, P. A., Patton, S., Lindsay, D. S., and Dubey, J. P. (2010) *Toxoplasma gondii*: epidemiology, feline clinical aspects, and prevention. *Trends Parasitol.* **26,** 190–196 CrossRef Medline
3. Xia, N., Ye, S., Liang, X., Chen, P., Zhou, Y., Fang, R., Zhao, J., Gupta, N., Yang, S., Yuan, J., and Shen, B. (2019) Pyruvate homeostasis as a determinant of parasite growth and metabolic plasticity in *Toxoplasma gondii*. *MBio* **10,** e00898-19 Medline
4. MacRae, J. I., Sheiner, L., Nahid, A., Tonkin, C., Striepen, B., and McConville, M. J. (2012) Mitochondrial metabolism of glucose and glutamine is required for intracellular growth of *Toxoplasma gondii*. *Cell Host Microbe* **12,** 682–692 CrossRef Medline
5. Blume, M., Rodriguez-Contreras, D., Landfear, S., Fleige, T., Soldati-Favre, D., Lucius, R., and Gupta, N. (2009) Host-derived glucose and its transporter in the obligate intracellular pathogen *Toxoplasma gondii* are dispensable by glutaminolysis. *Proc. Natl. Acad. Sci. U.S.A.* **106,** 12998–13003 CrossRef Medline
6. Krishnan, A., Kloehn, J., Lunghi, M., Chiappino-Pepe, A., Waldman, B. S., Nicolas, D., Varesio, E., Hehl, A., Lourido, S., Hatzimanikatis, V., and Soldati-Favre, D. (2020) Functional and computational genomics reveal unprecedented flexibility in stage-specific *Toxoplasma* metabolism. *Cell Host Microbe* **27,** 290–306.e11 CrossRef Medline
7. Ramakrishnan, S., Serricchio, M., Striepen, B., and Bütikofer, P. (2013) Lipid synthesis in protozoan parasites: a comparison between kinetoplastids and apicomplexans. *Prog. Lipid Res.* **52,** 488–512 CrossRef Medline
8. Coppens, I. (2013) Targeting lipid biosynthesis and salvage in apicomplexan parasites for improved chemotherapies. *Nat. Rev. Microbiol.* **11,** 823–835 CrossRef Medline

9. Ramakrishnan, S., Docampo, M. D., Macrae, J. I., Pujol, F. M., Brooks, C. F., van Dooren, G. G., Hiltunen, J. K., Kastaniotis, A. J., McConville, M. J., and Striepen, B. (2012) Apicoplast and endoplasmic reticulum cooperate in fatty acid biosynthesis in apicomplexan parasite *Toxoplasma gondii*. *J. Biol. Chem.* **287,** 4957–4971 CrossRef Medline
10. Ramakrishnan, S., Docampo, M. D., MacRae, J. I., Ralton, J. E., Rupasinghe, T., McConville, M. J., and Striepen, B. (2015) The intracellular parasite *Toxoplasma gondii* depends on the synthesis of long-chain and very long-chain unsaturated fatty acids not supplied by the host cell. *Mol. Microbiol.* **97,** 64–76 CrossRef Medline
11. Nolan, S. J., Romano, J. D., and Coppens, I. (2017) Host lipid droplets: an important source of lipids salvaged by the intracellular parasite *Toxoplasma gondii*. *PLoS Pathog.* **13,** e1006362 CrossRef Medline
12. Shears, M. J., Botté, C. Y., and McFadden, G. I. (2015) Fatty acid metabolism in the *Plasmodium* apicoplast: drugs, doubts and knockouts. *Mol. Biochem. Parasitol.* **199,** 34–50 CrossRef Medline
13. Mazumdar, J., and Striepen, B. (2007) Make it or take it: fatty acid metabolism of apicomplexan parasites. *Eukaryot. Cell* **6,** 1727–1735 CrossRef Medline
14. Foth, B. J., Stimmler, L. M., Handman, E., Crabb, B. S., Hodder, A. N., and McFadden, G. I. (2005) The malaria parasite *Plasmodium falciparum* has only one pyruvate dehydrogenase complex, which is located in the apicoplast. *Mol. Microbiol.* **55,** 39–53 Medline
15. Patel, M. S., Nemeria, N. S., Furey, W., and Jordan, F. (2014) The pyruvate dehydrogenase complexes: structure-based function and regulation. *J. Biol. Chem.* **289,** 16615–16623 CrossRef Medline
16. Park, S., Jeon, J. H., Min, B. K., Ha, C. M., Thoudam, T., Park, B. Y., and Lee, I. K. (2018) Role of the pyruvate dehydrogenase complex in metabolic remodeling: differential pyruvate dehydrogenase complex functions in metabolism. *Diabetes Metab. J.* **42,** 270–281 CrossRef Medline
17. Gray, L. R., Tompkins, S. C., and Taylor, E. B. (2014) Regulation of pyruvate metabolism and human disease. *Cell Mol. Life Sci.* **71,** 2577–2604 CrossRef Medline
18. McFadden, G. I. (2001) Chloroplast origin and integration. *Plant Physiol.* **125,** 50–53 CrossRef Medline
19. Fleige, T., Fischer, K., Ferguson, D. J., Gross, U., and Bohne, W. (2007) Carbohydrate metabolism in the *Toxoplasma gondii* apicoplast: localization of three glycolytic isoenzymes, the single pyruvate dehydrogenase complex, and a plastid phosphate translocator. *Eukaryot. Cell* **6,** 984–996 CrossRef Medline
20. Oppenheim, R. D., Creek, D. J., Macrae, J. I., Modrzynska, K. K., Pino, P., Limenitakis, J., Polonais, V., Seeber, F., Barrett, M. P., Billker, O., McConville, M. J., and Soldati-Favre, D. (2014) BCKDH: the missing link in apicomplexan mitochondrial metabolism is required for full virulence of *Toxoplasma gondii* and *Plasmodium berghei*. *PLoS Pathog.* **10,** e1004263 CrossRef Medline
21. Mazumdar, J., H Wilson, E., Masek, K., A Hunter, C., and Striepen, B. (2006) Apicoplast fatty acid synthesis is essential for organelle biogenesis and parasite survival in *Toxoplasma gondii*. *Proc. Natl. Acad. Sci. U.S.A.* **103,** 13192–13197 CrossRef Medline
22. Goodman, C. D., and McFadden, G. I. (2007) Fatty acid biosynthesis as a drug target in apicomplexan parasites. *Curr. Drug Targets* **8,** 15–30 CrossRef Medline
23. van Schaijk, B. C., Kumar, T. R., Vos, M. W., Richman, A., van Gemert, G. J., Li, T., Eappen, A. G., Williamson, K. C., Morahan, B. J., Fishbaugher, M., Kennedy, M., Camargo, N., Khan, S. M., Janse, C. J., Sim, K. L., *et al.* (2014) Type II fatty acid biosynthesis is essential for *Plasmodium falciparum* sporozoite development in the midgut of *Anopheles* mosquitoes. *Eukaryot. Cell* **13,** 550–559 CrossRef Medline
24. Vaughan, A. M., O'Neill, M. T., Tarun, A. S., Camargo, N., Phuong, T. M., Aly, A. S., Cowman, A. F., and Kappe, S. H. (2009) Type II fatty acid synthesis is essential only for malaria parasite late liver stage development. *Cell. Microbiol.* **11,** 506–520 CrossRef Medline
25. Hortua Triana, M. A., Márquez-Nogueras, K. M., Chang, L., Stasic, A. J., Li, C., Spiegel, K. A., Sharma, A., Li, Z. H., and Moreno, S. N. J. (2018) Tagging of weakly expressed *Toxoplasma gondii* Calcium-related genes with high-affinity tags. *J. Eukaryot. Microbiol.* **65,** 709–721 CrossRef Medline
26. Huynh, M. H., and Carruthers, V. B. (2009) Tagging of endogenous genes in a *Toxoplasma gondii* strain lacking Ku80. *Eukaryotic Cell* **8,** 530–539 CrossRef Medline
27. McFadden, G. I., and Yeh, E. (2017) The apicoplast: now you see it, now you don't. *Int. J. Parasitol.* **47,** 137–144 CrossRef Medline
28. Deleted in proof
29. Misra, A., Surolia, N., and Surolia, A. (2009) Catalysis and mechanism of malonyl transferase activity in type II fatty acid biosynthesis acyl carrier proteins. *Mol. Biosyst.* **5,** 651–659 CrossRef Medline
30. Misra, A., Sharma, S. K., Surolia, N., and Surolia, A. (2007) Self-acylation properties of type II fatty acid biosynthesis acyl carrier protein. *Chem. Biol.* **14,** 775–783 CrossRef Medline
31. Pei, Y., Tarun, A. S., Vaughan, A. M., Herman, R. W., Soliman, J. M., Erickson-Wayman, A., and Kappe, S. H. (2010) *Plasmodium* pyruvate dehydrogenase activity is only essential for the parasite's progression from liver infection to blood infection. *Mol. Microbiol.* **75,** 957–971 CrossRef Medline
32. Cobbold, S. A., Vaughan, A. M., Lewis, I. A., Painter, H. J., Camargo, N., Perlman, D. H., Fishbaugher, M., Healer, J., Cowman, A. F., Kappe, S. H., and Llinás, M. (2013) Kinetic flux profiling elucidates two independent acetyl-CoA biosynthetic pathways in *Plasmodium falciparum*. *J. Biol. Chem.* **288,** 36338–36350 CrossRef Medline
33. Shen, B., Brown, K., Long, S., and Sibley, L. D. (2017) Development of CRISPR/Cas9 for efficient genome editing in *Toxoplasma gondii*. *Methods Mol. Biol.* **1498,** 79–103 CrossRef Medline
34. Shen, B., Brown, K. M., Lee, T. D., and Sibley, L. D. (2014) Efficient gene disruption in diverse strains of *Toxoplasma gondii* using CRISPR/CAS9. *MBio* **5,** e01114-14 Medline
35. Xia, N., Yang, J., Ye, S., Zhang, L., Zhou, Y., Zhao, J., David Sibley, L., and Shen, B. (2018) Functional analysis of *Toxoplasma* lactate dehydrogenases suggests critical roles of lactate fermentation for parasite growth *in vivo*. *Cell Microbiol.* CrossRef
36. Long, S., Brown, K. M., Drewry, L. L., Anthony, B., Phan, I. Q. H., and Sibley, L. D. (2017) Calmodulin-like proteins localized to the conoid regulate motility and cell invasion by *Toxoplasma gondii*. *PLoS Pathog.* **13,** e1006379 CrossRef Medline
37. Ye, S., Xia, N., Zhao, P., Yang, J., Zhou, Y., Shen, B., and Zhao, J. (2019) Micronemal protein 13 contributes to the optimal growth of *Toxoplasma gondii* under stress conditions. *Parasitol Res.* **118,** 935–944 CrossRef Medline
38. Ecker, J., Scherer, M., Schmitz, G., and Liebisch, G. (2012) A rapid GC-MS method for quantification of positional and geometric isomers of fatty acid methyl esters. *J. Chromatogr. B Analyt. Technol. Biomed. Life Sci.* **897,** 98–104 CrossRef Medline